

FROM SENSOR TO DECISION: EVAPOTRANSPIRATION

DIRK V. BAKER, PhD

Historically, Campbell Scientific largely focused on the core technologies of designing and manufacturing data loggers, communications peripherals, and software as well as providing an open platform capable of integrating with a wide variety of sensors and sensing technologies. Over the last few years and ongoing into the future, Campbell Scientific started taking a more holistic approach, encompassing everything from increased attention to sensor development all the way to decision support. This approach includes data quality assurance and control, visualization, and other insights while maintaining the key strengths of our core technologies.

There is often a disconnect between measurement uncertainty at the sensor or measurement-system level and the end decisions made based upon those data.

This paper uses the calculation of evapotranspiration as an example to show how potential uncertainty in the measurements influences the estimate of evapotranspiration and, hence, decisions based upon that calculation.

First, a note on terminology. The terms “error” and “uncertainty” are often used interchangeably. This is generally acceptable and the semantics of the distinction between the two is outside the scope of this paper. However, in the specifications for sensors, the term used broadly in the industry is “accuracy.” Although technically incorrect, the term is so ingrained in manufacturing that it is unlikely to change. “Uncertainty” is the appropriate word and is the term used for the remainder of this paper.

Evapotranspiration

Evapotranspiration (ET) is defined as the movement of water from the soil into the atmosphere via evaporation and plant transpiration, and has units of depth (inches or millimeters)—the inverse of precipitation.

The key environmental variables driving ET include wind speed, solar radiation, air temperature, relative humidity, and vegetation type. The influence of the first four of these factors is intuitive: higher wind speeds, higher solar radiation, and higher air temperature all causing an increase in ET while increased relative humidity decreases ET (Figure 1).

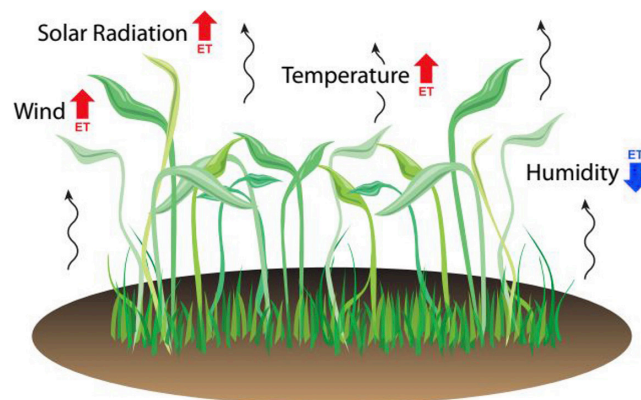


Figure 1: Schematic of evapotranspiration and the major contributing environmental factors

The influence of vegetation type is far more complicated and is typically only incorporated in a general way in the calculation. (I will discuss more of this later.) Applications for ET include decision-making for irrigation, research, and energy balance, among others.

The $ET_{sz}()$ instruction for Campbell Scientific data loggers uses the ASCE Standardized Reference hourly formulation of the Penman-Monteith (P-M) equation for ET (Allen et al. 2005).

$$ET_{sz} = \frac{0.408\Delta(R_n - G) + \gamma \frac{C_n}{T + 273} u_2 (e_s - e_a)}{\Delta + \gamma(1 + C_d + U_2)}$$

Where:

- Δ = slope of the saturation vapor pressure curve
- R_n = net radiation
- G = soil heat flux density
- γ = psychrometric constant
- C_n = numerator constant
- T = temperature
- u = wind speed
- e_s = saturation vapor pressure
- e_a = vapor pressure
- C_d = denominator constant

Nearly all these parameters are derived through a series of equations (more than 40 in total for the hourly calculation).

In this formulation, vegetation is treated as a height (short or tall) and is incorporated into an adjustment to wind speed based on the generalized vegetation height and the height of the wind speed observation (sensor mounting height). Vegetation height also accounts for leaf area and, therefore, differences in stomatal conductance.

The objective of this paper is to use real data and realistic sensor uncertainties to derive combined uncertainty estimates for ET. More specifically, the paper uses data from two sites in Utah, USA and specifications from three sensor combinations to examine potential uncertainty around the ET calculation.

Methods
Sites and Data

To compare impacts in somewhat different climates, two sites were chosen: one in southern Utah (near St. George) for a dry desert climate and one in northern Utah (Logan) where there is substantial surface water and irrigated pasture.

Data for the St. George site were obtained from MesoWest (<https://mesowest.utah.edu>) and the Logan data were from an ET107 operated by Campbell Scientific at the Logan office (Figure 2). Uncertainties were then added to these measurements based on hypothetical combinations of sensors (not necessarily the sensors used on those stations).

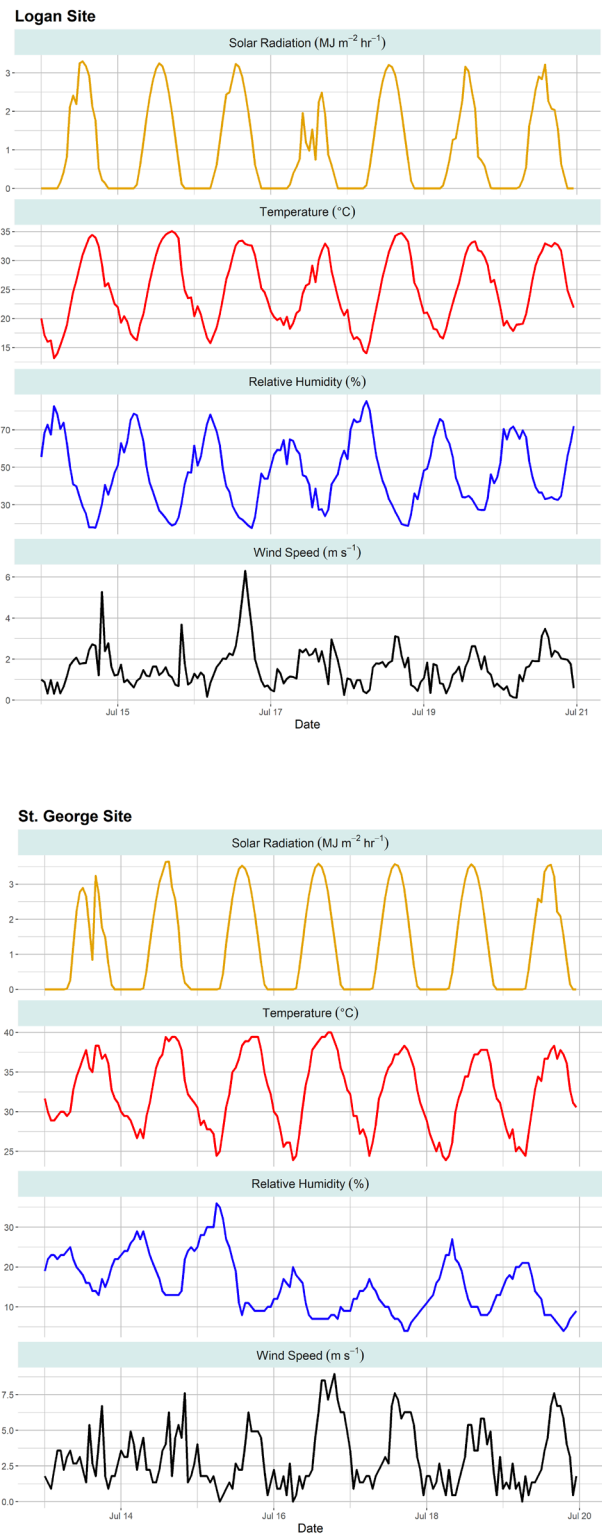


Figure 2: Data used as the basis for uncertainty estimation from two sites in Utah, USA

Table 1 shows the combinations of sensors used to base uncertainty estimates for combinations of high, medium, and low uncertainty. Published specifications for each of these sensors can be found on the Campbell Scientific website (<https://www.campbellsci.com/sensors>).

Table 1	High	Medium	Low
Temperature and Relative Humidity	HMP60	HygroVUE™10	HMP155A
Wind Speed	03002	05103	05103
Solar Radiation	CS301	CS320	CMP10

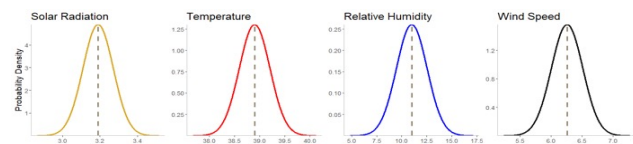
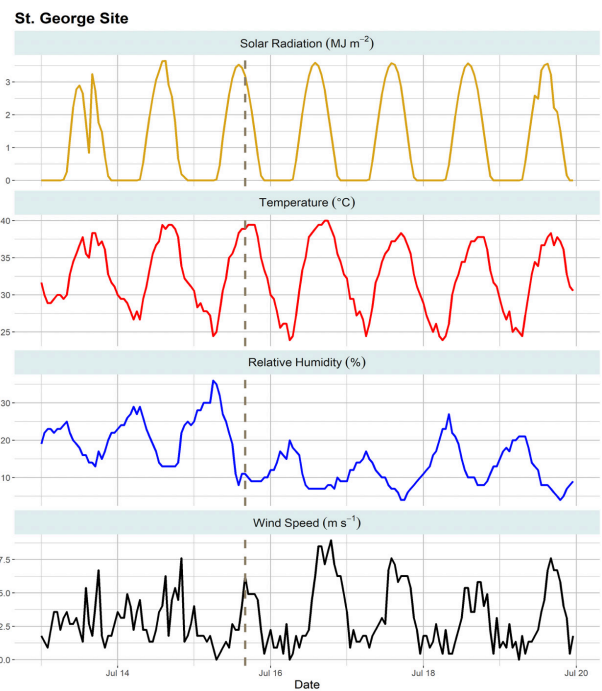
Uncertainty Estimation

To estimate the uncertainty of the ET calculation attributable to the sensors alone, a Monte Carlo method was used to combine the uncertainties of each sensor. The Monte Carlo method iteratively draws from a distribution to obtain aggregated results.

More specifically, for each sensor, the uncertainty was based on the published specifications with the key assumptions that the distribution of uncertainty was normal, and the specifications represented a 95% confidence interval. For each hourly time step in a given dataset, an error was added based on a random draw from a normal distribution centered at that data point.

The ET was calculated from the resulting wind, temperature, solar, and relative humidity data. This process was repeated 1,000 times for each site and each combination of sensors as well as for both short and tall reference vegetation to generate distributions of combined uncertainty for ET.

Figure 3a shows an example where the dotted vertical lines show time step. Figure 3b shows the assumed distribution around the respective data points from which points were randomly selected for that iteration of the process.

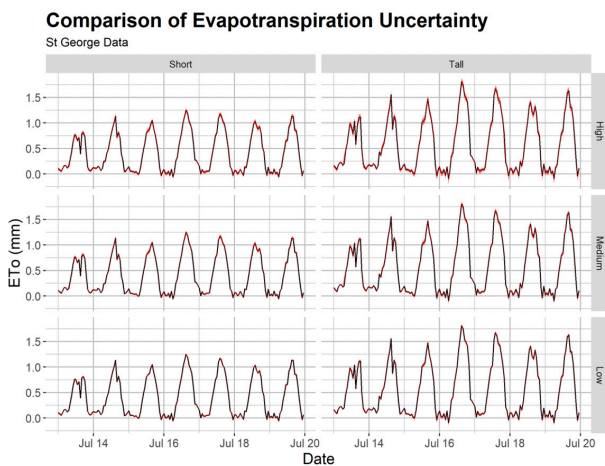
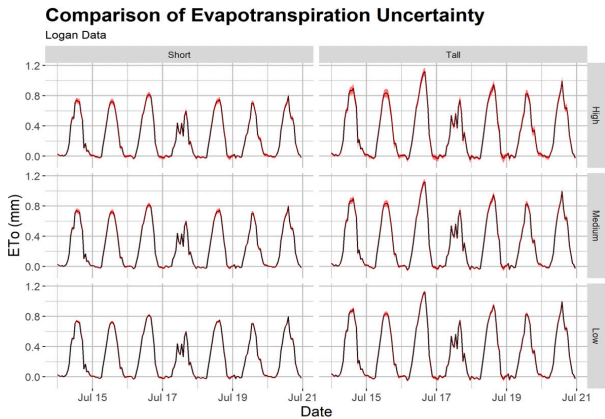


Figures 3a and 3b:

An illustration of a step in the iterative Monte Carlo uncertainty estimation process. The vertical dotted lines in 3a show a time step. The intersection of those lines with the weather data are shown in 3b, also as vertical dotted lines.

The normal distributions shown in 3b are based on the sensor specifications. For each step in the process, a point was randomly selected from these distributions to represent the measurement plus uncertainty.

Overall, less uncertainty was shown by these simulations for the calculated ET than expected (Figures 4a, 4b, and 5). However, there were cases that resulted in levels of uncertainty that are important whether the application is for irrigation decision-making, research, or otherwise. In addition, these uncertainties would be compounded over time.



Figures 4a and 4b:

Uncertainty estimations for each site (shown in red) are 95% intervals based on 1,000 iterations of each combination of site, reference vegetation height (short, tall), and sensor uncertainty level (high, medium, low – see Table 1). Black lines are ET calculated from the original data.

Not surprisingly, the influence of sensor selection is evident as is the impact of short versus tall reference (Figures 4a and 4b) with substantially greater uncertainty in ET for the sensors with greater uncertainty (lower accuracy). This uncertainty is also greater at the hotter, drier site in St. George than that in Logan.

The greatest maximum hourly uncertainty was 32%. This occurred with a combination of the St. George data, high uncertainty sensors, and tall reference vegetation. Maximum hourly uncertainties of greater than 10% occurred for 24 of the 84 combinations of site, sensor uncertainty level, reference type, and day of simulation; most of these occurred at the St. George site.

Interestingly, the maximum uncertainties for the daily summed ET showed a different pattern. In this case, for 3 of the 12 possible combinations of site, sensor uncertainty level, and reference vegetation, the maximum uncertainty was greater than 10% and two of these were with the Logan data. This is likely due to greater variability in the data and uncertainty at the St. George site.

The week’s total ET uncertainty was also maximized in the combination of high sensor uncertainty and tall reference vegetation at the St. George site (Figure 5).

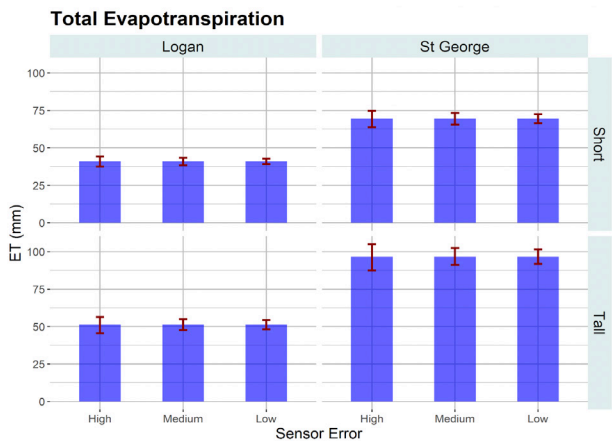


Figure 5:

Total ET (blue) calculated for the full week from the original data. The red bars represent 95% intervals based on 1,000 iterations of each combination of site, reference vegetation height (short, tall), and sensor uncertainty level (high, medium, low – see Table 1).

Several key assumptions and caveats are important to acknowledge. As mentioned, a normal distribution is assumed for the uncertainty of each sensor and further assumed that the published specifications represented a 95% confidence interval applicable to the full measurement range. This distribution has the effect that most of the time uncertainty is much smaller than the published specification and only rarely occurs at or near the specified limits.

Numerous potential distributions may be valid. Some simulations using a square distribution where the entire specified range of uncertainty were equally likely were also run (data not shown). Surprisingly, however, this did not substantially increase the uncertainty in ET. This suggests that, relative to other factors, the uncertainty in the sensors is small enough that different assumed distributions have little influence on the estimate of ET uncertainty.

Another key assumption is the P-M model itself. As mentioned previously, this model and its implementation (ASCE) is composed of many equations with their own sets of assumptions and there is a large body of research on the merits of the P-M model, its application, adjustments, and alternatives. These include substituting more direct measurements for some, or even all, of the equations. However, these can be cost prohibitive for some applications or large networks.

A final caveat to the generalization of these results is that the data were just one week from two sites, both in Utah, USA—a state largely characterized by various desert systems. There is also a great deal of active work examining the suitability of P-M for varying climates.

Closing Thoughts

The primary intent in this work was to use ET to illustrate a process to incorporate and account for the influence of measurement or sensor uncertainty on insights and decisions based on those data. This is not a common practice at least as presented to end users of data products. In fairness, it is not a simple practice either.

ET was chosen because it is commonly used in a variety of applications for research, ET products are commonly offered by large mesonets, and the calculation uses four common weather station measurements.

The results show remarkably little uncertainty in ET; though the uncertainties are probably important in at least some scenarios. This may, in part, result from the assumptions made about uncertainty distributions. Sensors may have smaller uncertainties than the specifications indicate.

There are published sensitivity analyses (e.g., Debnath et al., 2015)—studies that systematically vary model inputs to examine their influence on model results—that have shown greater effects than those in this work. However, the amount the inputs were varied was substantial, and I sought to use more realistic levels of uncertainty.

As Campbell Scientific continues to broaden its offerings to data products and decision support, incorporation and transparency around various uncertainties is a critical consideration.

References

1. Debnath, Subhankar, Sirisha Adamala, and N. S. Raghuvanshi. "Sensitivity Analysis of FAO-56 Penman-Monteith Method for Different Agro-Ecological Regions of India." *Environmental Processes* 2, no. 4 (2015): 689–704. <https://doi.org/10.1007/s40710-015-0107-1>.